LARGE MOMENTUM TRANSFER ELECTRON SCATTERING FROM FEW-NUCLEON SYSTEMS*

R. G. ARNOLD

The American University, Washington, D.C. 20016
and
Stanford Linear Accelerator Center, Stanford University,
Stanford, California 94305

ABSTRACT

A review is given of the experimental results from a series of measurements at SLAC of large momentum transfer ($Q^2 > 20$ fm^{-2}) electron scattering at forward angles from nuclei with $A \leq 4$. Theoretical interpretations of these data in terms of traditional nuclear physics models and in terms of quark constituent models are described. Some physics questions for future experiments are explored, and a preview of possible future measurements of magnetic structure functions of light nuclei at large Q^2 is given.

I. INTRODUCTION

Much of our knowledge of nucleon and nuclear structure has been derived from the electromagnetic structure functions measured in electron scattering experiments. The structure functions of the lightest nuclei ($A \leq 4$) are particularly important because they can be compared with our most precise microscopic theories. As the momentum transfer is increased, the energy and momentum from the virtual photon are deposited in a decreasing volume in the nucleus. The scattering cross sections at large Q^2 are expected to be sensitive to such features as: high momentum parts of the nuclear wave functions, relativistic kinematics, the effects of meson exchange and isobar currents, and eventually to the internal constituents of the nucleons.

II. THE DEUTERON

In our[1] first experiment[2] on electron-deuteron scattering, incident electrons with energies from 5 to 19 GeV were sent through a 30 cm long liquid deuterium target, and scattered electrons were measured at $8°$. Elastic cross sections were

---

(Presented at the International School of Intermediate Energy Nuclear Physics, Ariccia, Italy, June 18 - 27, 1979.)

measured in the momentum transfer range 0.8 to 6 GeV^2 (20 to 160 fm^{-2}) by detecting the scattered electrons in coincidence with the recoil deuterons using two large spectrometers. The coincidence detection method was crucial to the success of the elastic measurement and produced nearly background-free data down to cross sections of 10^{-38} cm^2/sr.

The cross section for elastic scattering is given by:

$$\frac{d\sigma}{d\Omega} = \sigma_{mott} \left[A(Q^2) + B(Q^2) \tan^2(\theta/2) \right] \quad . \quad (1)$$

Scattering at 8° measures the function $A(Q^2)$.

II.1. The Deuteron $A(Q^2)$

In the past two main goals of elastic ed scattering have been to differentiate between deuteron wave function models and to determine the neutron electric form factor G_{En} using the nonrelativistic impulse approximation (NRIA). The nucleon form factors enter $A(Q^2)$ through the isoscalar form factors squared. The largest contributions come from terms proportional to the square of the isoscalar electric form factor, $G_{ES} = G_{Ep} + G_{En}$. The proton electric form factor, G_{Ep}, is measured out to $Q^2 = 3$ GeV^2 (where the error is nearly 100%) and is consistent with the dipole shape. The neutron G_{En} is unknown above $Q^2 = 1$ GeV^2, and below that is very small, perhaps consistent with zero except for the slope at $Q^2 = 0$. The beating of the small G_{En} against the larger and generally better known G_{Ep} in the squared G_{ES} makes $A(Q^2)$ sensitive to small variations in G_{En}.

The deuteron $A(Q^2)$ at large Q^2 is, however, quite complicated, and straightforward tests of models of neutron structure and n-n potentials are not so easy. It is expected that at large Q^2 the meson exchange currents (MEC) and perhaps the isobar currents, caused by mutual excitation of the internal degrees of freedom of the nucleons, should make some contributions to the form factors. Also at large Q^2 a correct description of the scattering requires a relativistic treatment. At very large Q^2 (how large is very large?) the internal structure (quarks?) of the nucleons may determine the structure functions and a truly "first principles" calculation would start with the quark currents. To date there does not exist such a complete calculation, but we do have some advances to report.

II.2. Relativistic Impulse Approximation

There are several approaches, in the language of nuclear physics, to a relativistic impulse approximation (RIA) calculation of the deuteron structure functions. Two effects must be included: (a) relativistic kinematics, and (b) at least

one nucleon must be allowed to be off the mass shell. One method[3] is to start with covariant formulae and then transform away the negative energy states leaving results expressed in terms of corrections to some order in $(Q/m)^2$. F. Gross, in a series of papers,[4-6] has adopted an alternative approach where he keeps the negative energy states and makes a complete calculation including contributions from the small components of the deuteron wave function (P states).

The RIA calculation[5] begins with the covariant diagram of Figure 1(a), which includes the three time ordered diagrams of Figure 1(b) where the interacting nucleon is allowed to be off shell. This approach includes in a natural way to all orders in $(Q/m)^2$ or $(v/c)^2$ both the standard impulse terms and the terms where the photon splits into $n\bar{n}$, which are viewed in other language as the MEC pair terms. It does not include the genuine MEC currents of Figure 1(c) or the isobar currents of Figure 1(d). Four invariants are required to describe the npd vertex, and these can be written so they have the character of wave functions. Two of these functions are the familiar S and D state wave functions, u and w, present in the nonrelativistic treatment, and the two additional wave functions are P states associated with the extra degrees of freedom present when one nucleon is in the virtual Dirac states.
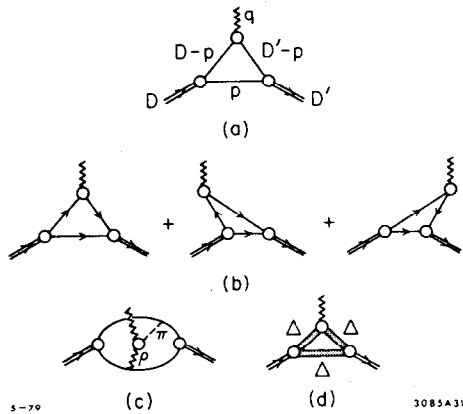

Figure 1. (a) The relativistic Feynman diagram of the impulse approximation, (b) three nonrelativistic time-ordered diagrams included in the RIA. Backward moving lines are anti-particles. (c) and (d) examples of two processes not included in the RIA. (c) a meson exchange diagrams, (d) the isobar contributions.

The relativistic formulae for the charge, quadrupole, and magnetic structure functions, G_C, G_Q, and G_M, are derived in a general way and can be evaluated with any deuteron wave functions. In particular if one chooses to neglect the P states, the formulae give the deuteron structure functions to all orders of $(Q/m)^2$ for any choice of u and w. A complete calculation requires a set of 4-component wave functions. The relativistic formulae have been evaluated numerically[5] using the deuteron models shown in Figure 2. The 4-component models, indexed by the mixing parameter λ, were obtained by Buck and Gross[6] from solutions to the relativistic wave equation. The P states are numerically small (0.5
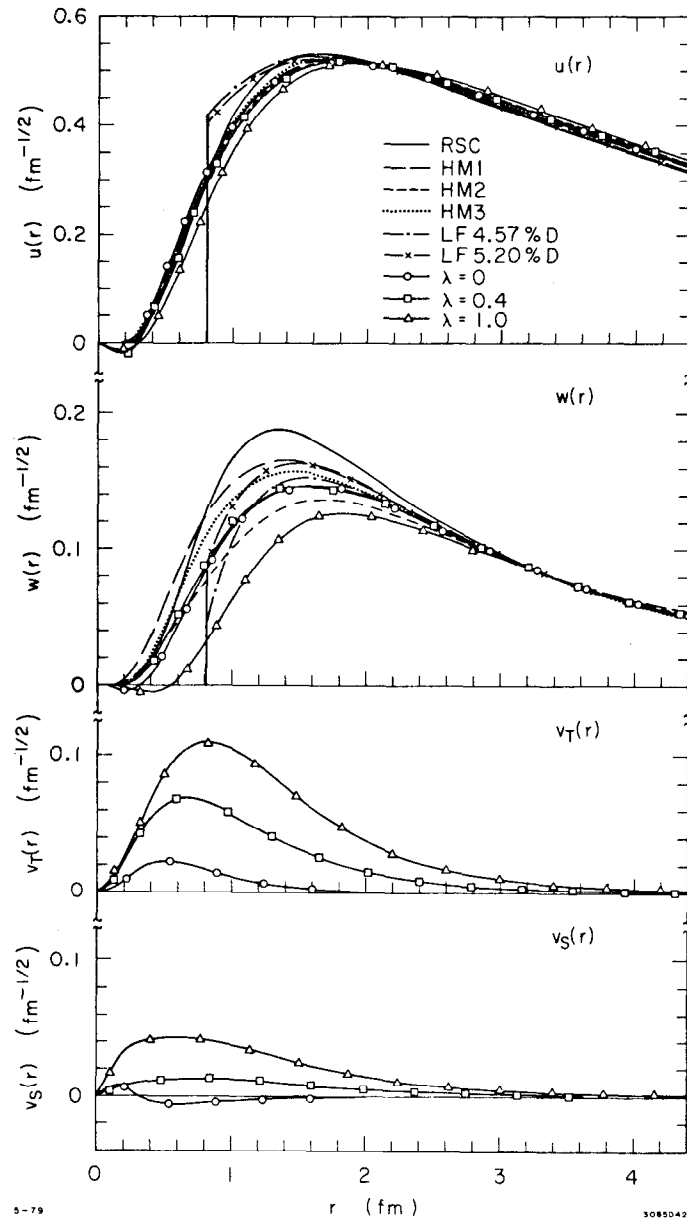
Figure 2. A collection of deuteron wave functions.
(a) The S state, (b) the D state, (c) and (d) the two
P states. The 2-component models are: Reid soft core
(Ref. 9), three Holinde-Machleidt models (Ref. 7), two
Loman-Feshbach models with different % D state (Ref. 8).
The 4-component Buck-Gross models (Ref. 6) are labeled
with the mixing parameter λ, which determines the form
of the π-n coupling. For $\lambda = 0$, the coupling is pure
$\gamma_5\gamma_\mu$, for $\lambda = 1$, it is pure γ_5.

to 2 percent of the total wave function), but at large Q^2 they can make appreciable contributions to the structure functions. All the models in Figure 2 have S states which are very similar, with the exception of the boundary condition models of Loman and Feshbach[8] which have a sharp discontinuity at 0.7 fm. The size and shape of the D states vary considerably, and it is primarily this variation which is reflected in the model dependence of the structure functions.

To investigate the effects of relativistic kinematics without the inclusion of the negative energy states, the relativistic formulae were evaluated using the 2-component models in Figure 2. The results for $A(Q^2)$ using dipole nucleon form factors with $G_{En} = 0$ are presented in Figure 3. The

effects of relativistic kinematics on $A(Q^2)$ are shown in more concise form in Figure 4 where the ratio of the relativistic to the nonrelativistic results are plotted. The relativistic kinematic correction decreases the value of $A(Q^2)$ out to Q^2 about 140 fm^{-2}, and this correction is fairly model independent out to Q^2 of approximately 100 fm^{-2}. The effect on the individual form factors G_C, G_Q, and G_M is generally to shift the position of diffraction minima to lower Q^2 and increase the height of the following maxima.
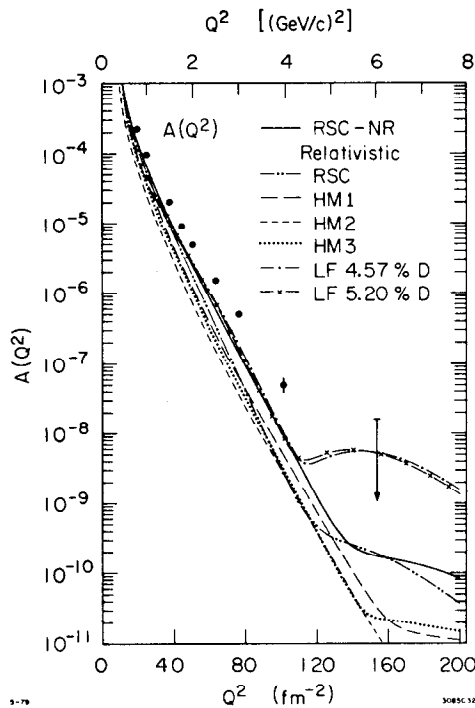
Figure 3. The deuteron elastic structure function $A(Q^2)$ evaluated in the RIA using the 2-component models in Figure 2. The curve RSC-NR, determined from the nonrelativistic Reid soft core model, is presented for comparison. Dipole nucleon form factors were used with $G_{En} = 0$.

Figures 3 and 4 reveal the basic problem with $A(Q^2)$ in the RIA using dipole form factors with $G_{En} = 0$. All the models give results which fall below the data by factors of 2 to 10. The overall effect of relativistic kinematics is to depress the nonrelativistic results and further widen the difference between the data and theory.
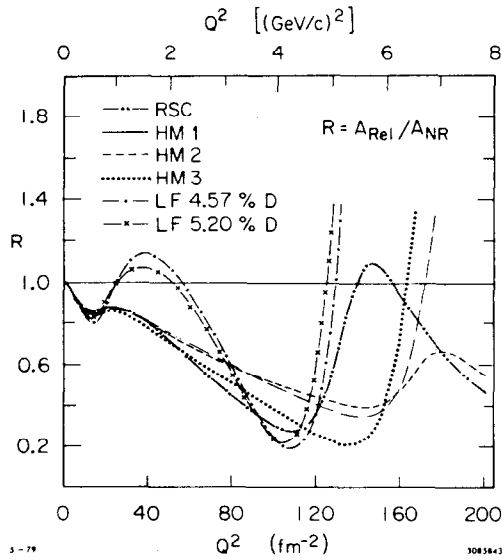
Q^2 [(GeV/c)^2]

```
        RSC
        HM 1              R = A_Rel / A_NR
        HM 2
        HM 3
        LF 4.57 % D
        LF 5.20 % D
```

Q^2 (fm^{-2})

Figure 4. Relativistic kinematic corrections to the structure function $A(Q^2)$. The ratio of A calculated using the RIA formulae to A calculated using the nonrelativistic formulae is given for each 2-component model in Figure 2.

Results for $A(Q^2)$ using three of the Buck-Gross 4-component models[6] are plotted together with the Reid soft core nonrelativistic (RSC-NR) result in Figure 5. The P states tend to have the opposite effect of the relativistic kinematics, i.e., they shift diffraction minima to higher Q^2 and lower the height of 2nd diffraction maxima. The present uncertainty in the form of the off shell π-n coupling will be eliminated when the n-n phase shift data are analysed using the Gross relativistic formalism.

Figure 5. The deuteron elastic structure function $A(Q^2)$ evaluated in the RIA using three of the 4-component models from Ref. 6. The RSC-NR curve is the nonrelativistic Reid soft core result. Dipole nucleon form factors were used with $G_{En} = 0$.

Q^2 [(GeV/c)^2]

$A(Q^2)$

```
        RSC - NR
        λ = 0
        λ = 0.4
        λ = 1.0
```

Q^2 (fm^{-2})
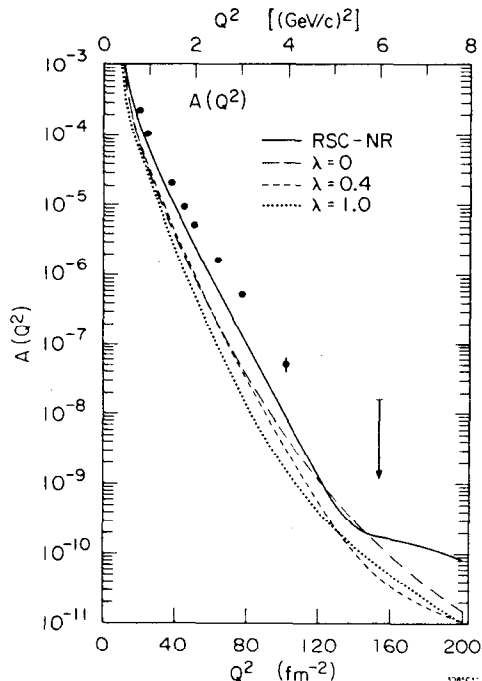
II.3. The Neutron G_{En}

We have also investigated the sensitivity of $A(Q^2)$ to various choices for the neutron G_{En}. In Figure 6 is an example of $A(Q^2)$ evaluated with 5 different versions of G_{En} displayed in Figure 7. The results for the dipole form with $G_{En} = 0$ are too low as described above. The IJL parameterization[10] for G_{En} was determined from a fit to the neucleon form factor data excluding G_{En} in a vector dominance model. Their result for G_{En} goes through zero and becomes negative above $Q^2 = 38$ fm^{-2} with absolute value comparable to G_{Ep}. Therefore G_{ES} goes through a sharp minimum at
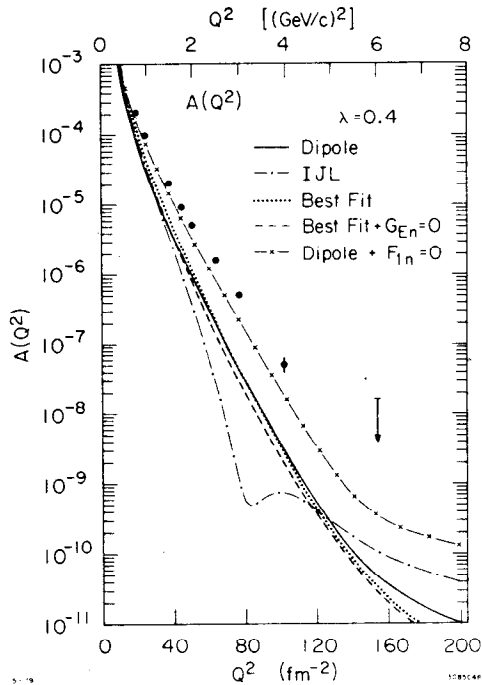

Figure 6. The deuteron $A(Q^2)$ evaluated in the RIA using the 4-component model with $\lambda = 0.4$ and five versions of the neutron structure function G_{En} presented in Figure 7.

Figure 7. Various estimates for the neutron structure function G_{En}. The curves are: Best Fit, from Galster et al. (Ref. 12); IJL from Ref. 10; and $F_{1n} = 0$ leading to the form given in Eq. 2. For comparison the dipole curve for G_{Ep} is also shown.
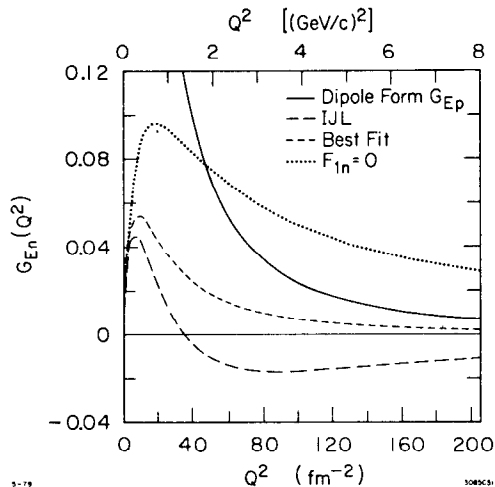
about 85 fm^{-2}, which introduces a sharp dip in the structure functions in that region in addition to those due to the body form factors. As Figure 6 indicates, the data for $A(Q^2)$ seem to eliminate the possibility of such a dip.

As an example of what we regard as a more reasonable neutron form factor, we used a collection of nucleon form factors we call "Best Fit".[11] It is not the result of a comprehensive fit but each curve does accurately represent the available data. The G_{En} is taken from the fit by Galster et al.[12] To display the sensitivity of $A(Q^2)$ to variations in G_{En} around zero, we have plotted in Figure 6 two Best Fit curves, one with and one without G_{En} set to zero. Finally, the curve labeled "Dipole + $F_{1n} = 0$" is an attempt to indicate what possible form G_{En} could take to give agreement with the $A(Q^2)$ data. The assumption that the Dirac form factor F_{1n} is equal to zero is consistent with the prediction of the symmetric quark model where the nucleon valence quarks are all in a spacially symmetric ground state. This gives, with $\tau = Q^2/4M_n^2$

$$G_{En} = \tau G_{Mn} = -\mu_n \tau\, G_{Ep} \qquad (2)$$

The resulting curve for G_{En} in Figure 7 is about a factor of two higher than the Best Fit value, and is at the upper edge of the large experimental[12] error bars in the Q^2 range up to 1 GeV^2.

From Figure 6 we conclude that it is possible, assuming for the moment that genuine MEC contributions can be ignored, to get fairly good agreement with the data using reasonable values for G_{En}. However, the genuine isoscalar MEC[30] (Figure 1(c)) may also be important at large Q^2, and a straightforward deduction of G_{En} from this calculation is not possible.

II.4. Observations on the deuteron $A(Q^2)$

To summarize, the deuteron $A(Q^2)$ at large Q^2 presents a rather complicated problem. The overall size of the feature-less curve depends in a complex way on many ingredients. The individual form factors G_C, G_Q, and G_M have sharp diffractive features that are sensitive to the details of the models, but unfortunately this sharp structure is completely obscured in the total $A(Q^2)$. At present all the reasonable two-body potential models give NRIA results for $A(Q^2)$ which are systematically too low when dipole nucleon form factors are used with $G_{En} = 0$. This deviation is increased when relativistic kinematics are used. The uncertainty in $A(Q^2)$ from uncertainty in the size of G_{En} is large and could possibly account for most of the discrepancy. The main outstanding problem is the inclusion of the genuine MEC contributions (Figure 1(c)) in a comprehensive relativistic treatment.

III. HELIUM

Electron scattering from ^{3}He and ^{4}He at large Q^2 was recently measured[13] at SLAC in a manner similar to that for the deuteron with elastically scattered electrons detected at 8° in coincidence with the recoil nuclei. For elastic scattering at small angles, the cross section for ^{3}He is given mostly by the function $A(Q^2)$, which in terms of the charge F_{ch} and magnetic F_{mag} form factors is:

$$A(Q^2) = \left[F_{ch}^2 + \mu^2 \tau F_{mag}^2 \right] \Big/ (1 + \tau) \qquad (3)$$

For the spin zero ^{4}He, $A^{\frac{1}{2}} = F_{ch}$.

Prior to this experiment there existed something of a crisis in the 3-body problem. Using any of the realistic n-n potentials in Faddeev or variational 3-body calculations does not give good agreement with the ^{3}He charge form factor. The theoretical minima are at too large Q^2 and the height of the second maxima are too small by factors of 3 to 4. This situation is somewhat improved by the addition of the MEC corrections,[17,18] but still the disagreement persists and is regarded as a serious problem.

The present situation in ^{3}He is summarized in Figure 8. The Faddeev calculations[15,16] give F_{ch} a factor of 4 to 10 below the data from Q^2 0.8 to 2 GeV^2. These theories predict a 2nd diffraction minimum around $Q^2 = 2$ GeV^2, but it is not possible to state clearly that such a feature is visible in
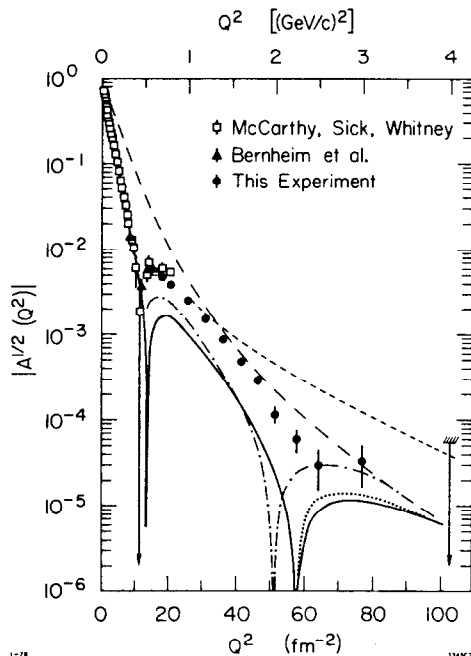

Figure 8. ^{3}He $A^{\frac{1}{2}}$ data at large Q^2 (Ref. 13), together with previous data (Ref. 14), and theoretical predictions for F_{ch} and $A^{\frac{1}{2}}$. The curves are: solid, F_{ch} Faddeev (Ref. 15); dotted, F_{ch} Faddeev (Ref. 16); dot-dashed, Faddeev (Ref. 15) plus MEC (Ref. 17); small dashed, $A^{\frac{1}{2}}$ DSQM (Ref. 19); large-dashed, $A^{\frac{1}{2}}$ RIA (Ref. 20).

the new data. One difficulty with the interpretation of Figure 8 is that the theoretical contributions for F_{mag} at large Q^2 were not available at the time that figure was prepared, and F_{mag} is not measured beyond $Q^2 = 0.8$ GeV^2. A recent calculation[21] of F_{mag} using several n-n potentials in a variational approach indicates that above $Q^2 = 2$ GeV^2, F_{mag} is the dominant term in $A(Q^2)$, completely altering the shape of the 2nd diffraction feature from F_{ch}. The total $A(Q^2)$ is, however, still too low by factors of 2 to 4 in the Q^2 region 0.8 to 2 GeV^2, which remains as a serious problem.

I. Sick has made the observation[22] that the height of the second maximum in the ^{3}He F_{ch} is correlated with a dip in the nuclear charge density (also in the one-body density) near the origin, this is not predicted in the Faddeev and variational calculations. This disagreement could indicate that either there is not enough repulsion in the present models of the interaction between pairs of nucleons at short distances, or that there are three-body interactions that introduce correlations which somehow push the protons away from the origin This would give more of a squared-off edge at the nuclear radius which would enhance the size of the second diffraction maxima. The overall situation[13] in ^{4}He F_{ch} is similar to that for ^{3}He. The present few-body calculations based on realistic n-n potentials, while admittedly in a more primitive state than for the 3-body case, give F_{ch} with second maxima that are too low by factors of 3 to 4. For ^{4}He there is no F_{mag} to confuse the issue.

IV. ASSYMPTOTIC FORM FACTORS - QUARKS IN NUCLEI

It is fairly evident now that nucleons are in some sense made of pointlike charged constituents. The general picture of hadron structure emerging from recent discoveries at e^+e^- storage rings and the growing body of deep inelastic and high transverse momentum data is one of colored quarks of various flavors bound via exchange of colored gluons into the familiar hadrons as color singlets. The gauge theory of colored quarks and gluons, quantum chromodynamics (QCD), is emerging as the underlying theory of strong interactions. The long range attraction between quarks leading to the apparent confinement of the color fields is not understood, but at short distances the interactions are weak (asymptotic freedom) and perturbation theory works.

The growing confidence in the QCD model for hadron structure leads to the possibility that the long-standing questions about the n-n interaction at short distances may be soon understood in terms of a fundamental theory. In the nuclear physics picture, nucleons are usually considered as elementary fermions moving in the nuclear potential and surrounded by clouds of mesons. The nucleon internal structure is treated phenomeno-

logically in terms of various form factors. The nuclear
potential is pictured to arise from the exchange of various
numbers and types of mesons with the long range interaction
described well by the one-pion-exchange potential (OPEP).
In the quark picture, the nucleons are tightly bound color-
singlet states of colored quarks and gluons. Nucleons inter-
act by exchanging quarks and gluons. At short distances the
meson exchange picture becomes uneconomical because too many
complex exchanges of heavy mesons are required to give an
adequate description of the very complicated interactions.
At long range (r > 1 fm) the quark picture is not so useful
because in that region the nonperturbative and poorly under-
stood long range attraction between quarks which binds them
into mesons and nucleons must be taken into account. For n-n
interactions at separations less than 1 fm, the nucleons
(radius ∼0.9 fm) strongly overlap and the quarks intermingle.
In this overlap region, which is probed by high momentum
transfer experiments, the quark currents may be a more useful
basis for a description of the structure than the phenomeno-
logical meson currents. At intermediate Q^2 the two pictures
should be complimentary.

There are several approaches to quark models of nuclear
structure. The dimensional scaling quark model (DSQM)[19] was
developed mainly in an attempt to understand the large body
of high energy and large transverse momentum data. The pri-
mary predictions of the model are that hadronic elastic and
inelastic structure functions fall with increasing momentum
transfer, Q^2, according to powers of Q^2, where the power is
determined by counting the number of quarks participating in
the reaction. The quark counting rules and powerlaw fall off
of structure functions follows from the underlying scale in-
variant interaction of the pointlike constituents at short
distances. The DSQM predicts the shape of (spin averaged)
electromagnetic form factors, which are a special case of the
general structure functions, to fall with a power of Q^2 like

$$A^{\frac{1}{2}} = F_H \sim \left(\frac{1}{Q^2}\right)^{n-1} \tag{4}$$

where n is the number of quarks in the hadron. One additional
power of Q^2 is required in the form factor for each quark that
must change momentum in the scattering.

What evidence do we have for the power law fall off of
hadronic form factors? In Figure 9 are plotted the world's
data for the hadron form factors for A ≤ 4 divided by the
DSQM prediction. The π and proton data closely follows the
predicted power law behavior. The deuteron appears to be
approaching the asymptotic shape above $Q^2 = 4$ GeV^2, while the
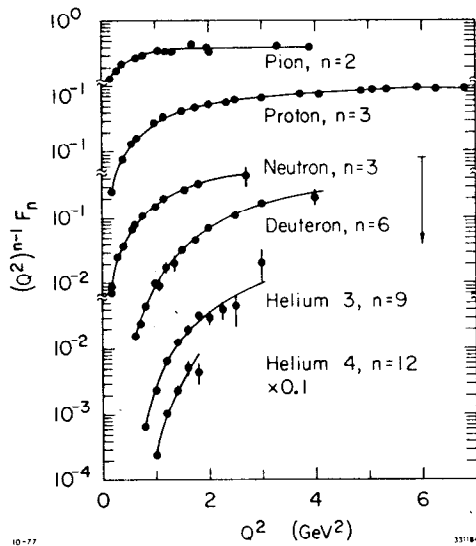^{3}He and ^{4}He data are so far known only in the preasymptotic

Figure 9. Elastic electromagnetic form factors of hadrons and nuclei with $A \leq 4$ for large Q^2, divided by the DSQM model. The curves simply connect the data points.

region. These curves suggest that somewhere in the region of $Q^2 = 4$ to 6 GeV^2 the nucleon quark constituents determine the shape of the nuclear structure functions.[23]

The quark counting models are able to predict only the shape of the hadronic structure functions. What we really would like is a complete calculation of the shape and size of the form factors beginning with the quark currents. Brodsky and co-workers[24] have recently derived the DSQM power law predictions for exclusive (elastic) scattering processes at large Q^2 in a perturbative type QCD model. Their results give meson and nucleon form factors which contain the power law terms of the DSQM, plus terms containing logarithms of the QCD coupling constant that give small violations of perfect scaling at large Q^2. They suggest that exclusive form factors at large Q^2 are a prime testing ground for the predictions of QCD, for example, in the proton above Q^2 of 4 GeV^2. It is unlikely that clear tests of perturbative QCD will be made at the relatively low Q^2 attainable in scattering from nuclei. However, such data will clearly bear on the collective aspects of QCD and will illuminate the transition to the region where perturbation theory and the scaling ideas work.

Another approach to nuclear structure in the quark model is in the context of the so-called bag models,[25-27] in particular the recent work[25] by C. DeTar. He has studied the interaction of six quarks with the isotopics of the deuteron in the MIT bag model. He used the static cavity approximation and looked at the total energy of the system as the separation between the centers of mass of the neutron and proton quarks was varied. The important result is that the total energy has a minimum for nucleon separations around 0.8 fm and rises at larger separation due to the color-electric force. At small separations in the region of the repulsive core, the energy rises due to the color-magnetic interaction between the quarks.

DeTar has recently extended[26] this work and he gets directly the correct sign for the tensor force and the deuteron quadrupole moment from the basic quark-quark interactions.

So far the bag model is not able to produce deuteron form factors at large Q^2 because it is not clear yet how to do dynamical calculations to include such phenomena as bag surface oscillations and recoil of the bag system. Also, the long range interaction between bags, which should reproduce the well established OPEP interaction, is not treated in the MIT models. Some of these problems are being actively investigated.[27] It is evident from the bag model studies and the QCD calculations of asymptotic form factors that the old questions about the nature of the n-n interaction inside 1 fermi are being explored from exciting new points of view. These investigations will undoubtedly be extended in the near future, and could eventually lead to a comprehensive theory of nucleon interaction starting with the quark currents. It is also clear that probes of the electromagnetic currents in the few nucleon systems by large Q^2 electron scattering will provide crucial evidence necessary to shape the development of these ideas.

V. QUESTIONS FOR FUTURE EXPERIMENTS

There are several options for future experiments in this area. More data for $A(Q^2)$ at larger Q^2 is not a likely possibility. The present limits, determined by low cross sections, are at the edge of feasibility for the present generation of accelerators, spectrometers, and targets. The ultimate limits are set by geometry (solid angles) and the tolerance of targets and detectors for high rates. There are perhaps factors of 2 to 10 to be gained with clever design and lots of money, but not two or three orders of magnitude.

Separation of the deuteron G_C and G_Q would be of enormous importance in untangling the present confusion in $A(Q^2)$. There are two possible experimental methods. In one case, unpolarized electrons are scattered from a polarized target, and in the other the distribution of polarization of the recoil deuterons following scattering from unpolarized electrons must be measured. Figure 10 shows the recoil deuteron tensor polarization,[28] $T(Q^2)$, calculated[5] using the RIA and various 2-component models. In the recoil tensor polarization, G_C and G_Q are beat together giving a curve sensitive to the diffractive shapes, particularly the shape of G_C. To first order $T(Q^2)$ is independent of the nucleon form factors. The model dependence evident in Figure 11 is mostly due to variations in the shape of the D state, and one might hope that a measurement of $T(Q^2)$ around $Q^2 = 1$ GeV^2 would be decisive in discriminating between potential models. However, the size of the P states in the relativistic treatment also make similar variations in $T(Q^2)$, and it can be expected that the MEC will
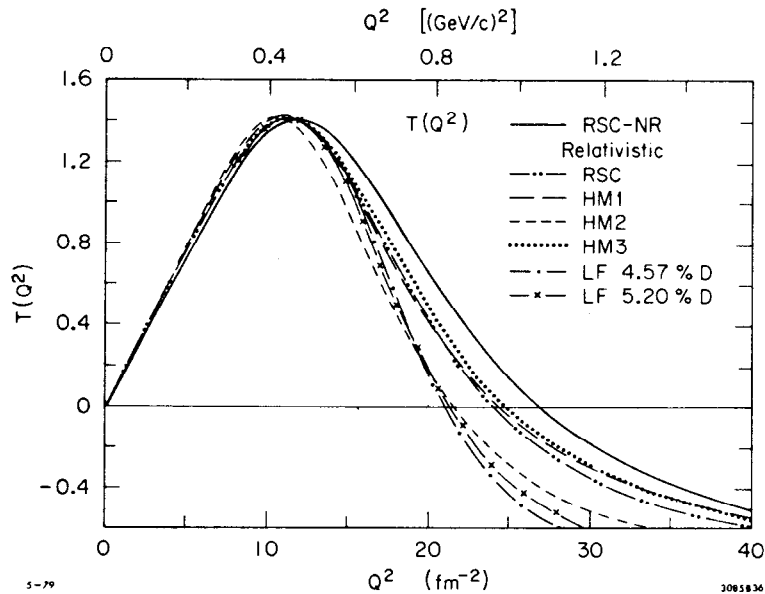
Figure 10. The deuteron recoil tensor polariza-
tion $T(Q^2)$ evaluated using the relativistic
formulae of Ref. 5 and the 2-component deuteron
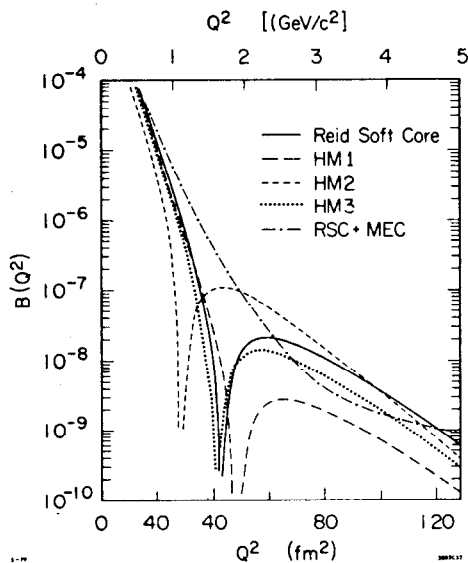models displayed in Figure 2.

Figure 11. The deuteron
elastic structure func-
tion $B(Q^2)$ evaluated in
the NRIA with dipole
nucleon form factors and
various 2-component deu-
teron models. The curves
are: RSC (Ref. 9); HM_1,
HM_2, and HM_3 (Ref. 7);
RSC + MEC Reid soft core
plus meson exchange
(Ref. 30).

also have similar sized effects. Therefore, a measurement of $T(Q^2)$, while it would certainly give added constraints, would probably only narrow the choices rather than make clear distinctions between models.

Unfortunately, there does not now exist a technology for either polarized deuteron targets which can stand the high beam currents necessary for low cross section measurements, or a deuteron polarimeter with known analyzing power for use at large recoil momentum. Separation of G_C and G_Q will await developments in these fields.

Another possibility is to measure the magnetic structure functions at large Q^2 by doing backward angle electron scattering.[29] The $B(Q^2)$ functions of the light nuclei can be easily isolated experimentally, and in the impulse approximation they are expected to show sharp diffractive features in the Q^2 region 0.8 to 2 GeV^2. The exact position of the minima and the height of the second maxima are strongly related to such properties as the shape of the D state, the nature of the π-n coupling, and the presence of the exchange currents. For example, in the calculation of Gari and Hyuga[30] for the deuteron, the MEC completely alter the shape of the NRIA diffractive features in $B(Q^2)$ by filling in the minimum around 40 fm^{-2}. Some of the nonrelativistic predictions for the deuteron $B(Q^2)$ are shown in Figure 11. The present measurements[2] extend only out to $Q^2 = 25$ fm^{-2} where the experimental error is nearly 100%.

The predictions for large isoscalar MEC effects in the deuteron $B(Q^2)$ can be compared to the similar effect of the isovector MEC on the electrodisintegration cross section at threshold in the same Q^2 range. In practice any measurement of $B(Q^2)$ will be accompanied almost for free by a measurement of the inclusive spectra. A direct comparison of the elastic and threshold inelastic cross sections at large Q^2 could place storng constraints on possible MEC currents.

Several predictions[18,31] are available for F_{mag} in ^{3}He and ^{3}H. Barroso and Hadjimichael[31] indicate, for example, that the interference between the S and D state parts of the 3-body wave functions cause the location of the diffraction minima in ^{3}He and ^{3}H F_{mag} to shift down in Q^2 by 6 fm^{-2} in the Q^2 region 8 to 20 fm^{-2}, while the MEC contributions shift them back toward higher Q^2 by comparable amounts. The structure functions of d, ^{3}He and ^{3}H are all tightly interconnected. Comparison of high Q^2 magnetic structure function measurements in all these nuclei would put strong limits on the models, and could perhaps give a clue to the source of the current problems in the $A(Q^2)$ functions.

VI. POSSIBLE FUTURE EXPERIMENTS

We are proposing[29] to measure elastic and inelastic magnetic structure functions of the light nuclei in the Q^2 range 0.6 to approximately 2 GeV^2 at SLAC using 30 to 40 cm long targets and the Rosenbluth method at angles from 35° to 155°. The cross sections are expected to fall to the level of 10^{-36} to 10^{-40} cm^2/sr in that Q^2 range, and it is absolutely necessary to have high beam intensities in the energy range 0.5 to approximately 2 GeV and to use thick targets to achieve appreciable counting rates.

To provide a high intensity electron beam we are proposing to build an off-axis gun and in-line injector at Section 26 of the 30-Sector linac. The new beam could have a maximum (unloaded) energy of 3.5 GeV and a maximum duty factor of 5.7 × 10^{-4} at 360 pps with a 1.6 µs pulse length. At 100 mA peak current, the beam loading would reduced the maximum energy to 2.9 GeV. By installing the new injector near the output end of the linac, it will be possible to deliver beams with intensity increased 10 to 50 times over what is presently available at SLAC in that energy range due to the shortened length of accelerator contributing to beam breakup.

This new beam will fill an energy gap in high intensity, low duty factor electron beams for nuclear structure physics between the range of the Bates-Saclay-IKO machines and the present high energy SLAC beams. The low duty factor limits the use of the new beam to single arm inclusive reactions or to highly correlated (elastic) coincidence measurements. We are also considering for possible future proposals to add a radio-frequency energy compression system that could compress the momentum spectrum of the beam to a spread of .01% dp/p. For the present we propose to do elastic scattering in coincidence using two large SLAC spectrometers, and also to do a longitudinal-transverse separation in the threshold and the quasielastic region in single arm measurements. This data would cover the Q^2 region expected to contain sharp diffractive features discussed above, and would be important evidence to guide our ideas about the nucleon-nucleon interaction at separations inside 1 fm and about the meson presence in nuclei.

VII. CONCLUSIONS

Data on electromagnetic form factors of light nuclei at large Q^2 are uniquely available from experiments using high intensity, high energy electron beams, and they can be readily performed using the present generation of low duty factor accelerator. High Q^2 measurements probe the nuclear systems in the region of overlap between nuclear and quark physics, and such data will compliment the new results at lower Q^2

soon to come from more complicated coincidence experiments
using the next generation of lower energy, but higher duty
factor, accelerators now being developed in laboratories
around the world.

VIII. REFERENCES

1. The present and past members of and collaborators with
   the American University Group at SLAC are: R. Arnold,
   B. Chertok, E. Dally, D. Day, A. Grigorian, C. Jordan,
   F. Martin, J. McCarthy, B. Mecking, S. Rock, I. Schmidt,
   W. Schütz, I. Sick, Z. Szalata, G. Tamas, R. York and
   R. Zdarko.

2. R. Arnold et al., Phys. Rev. Lett. 35, 776 (1975), F.
   Martin et al., Phys. Rev. Lett. 38, 1320 (1977).

3. J. Friar, Ann. Phys. (N.Y.) 81, 332 (1973); Phys. Rev.
   C12, 695 (1975).

4. F. Gross, Phys. Rev. D10, 223 (1974) and references
   therein.

5. R. Arnold, C. Carlson and F. Gross, SLAC-PUB-2318, to
   be submitted for publication.

6. W. Buck and F. Gross, Phys. Lett. 63B, 286 (1976), and
   William and Mary Preprint 78-9, to be published in Phys.
   Rev. D.

7. K. Holinde and R. Machleidt, Nucl. Phys. A256, 479 (1976),
   Nucl. Phys. A256, 497 (1976).

8. E. Loman and H. Feshbach, Ann. Phys. (N.Y.) 48, 94 (1968).

9. R. Reid, Ann. Phys. (N.Y.) 50, 411 (1968).

10. F. Iachello, A. Jackson and A. Lande, Phys. Lett. 43B,
    191 (1973).

11. The Best Fit nucleon form factors were first used and
    are described in detail in Ref. 2.

12. S. Galster et al., Nucl. Phys. B32, 221 (1971).

13. R. Arnold et al., Phys. Rev. Lett. 40, 1429 (1978).

14. J. S. McCarthy et al., Phys. Rev. C15, 1396 (1977) and
    references therein.

15. R. Brandenburg et al., Phys. Rev. C12, 1368 (1975).

16. A. Laverne and C. Gignoux, Phys. Rev. Lett. 29, 436 (1972).

17. J. Borysowicz and D. Riska, Nucl. Phys. A254, 301 (1975).

18. E. Hadjimichael, Nucl. Phys. A294, 513 (1978); M. Haftel,
    W. Kloet, Phys. Rev. C15, 404 (1977) and references
    therein.

19. The DSQM model is the work of many people. See S. Brodsky and B. Chertok, *Phys. Rev. D14*, 3003 (1976) and references therein.

20. I. Schmidt and R. Blankenbecler, *Phys. Rev. D15*, 3321 (1977), *Phys. Rev. D16*, 1318 (1977).

21. T. Katayama, Y. Akaishi and H. Tanaka, Hokkaido University Preprint HOUP-78118, Japan (1978).

22. I. Sick, Proceedings of Workshop on Few Body Systems and Electromagnetic Interactions, Frascati, 1978.

23. See also B. Chertok, *Phys. Rev. Lett. 41*, 1155 (1978).

24. S. Brodsky, G. Lepage, SLAC-PUB-2294 and references therein.

25. C. DeTar, *Phys. Rev. D17*, 302 (1978), and *D17*, 323 (1978).

26. C. DeTar, *Phys. Rev. D19*, 1451 (1979).

27. G. Brown and M. Rho, *Phys. Lett. 82B*, 177 (1979); C. Carlson, F. Myhrer and G. Brown, NORDITA preprint 79/15 (1979).

28. M. Moravcsik and P. Ghosh, *Phys. Rev. Lett. 32*, 321 (1974) and references therein.

29. R. Arnold et al., Proposal for Measurement of Electron-Deuteron Elastic and Inelastic Magnetic Structure Functions at Large Momentum Transfer, SLAC Experiment E134 (1978).

30. M. Gari and G. Hyuga, *Nucl. Phys. A264*, 409 (1976), and *Nucl. Phys. A278*, 372 (1977).

31. A. Barroso and E. Hadjimichael, *Nucl. Phys. A238*, 422 (1975).